With use of an in vitro sciatic nerve incubation, compounds were tested for their ability to inhibit sorbitol accumulation in isolated tissue. Sciatic nerves from rats (Sprague-Dawley) were quickly removed and incubated for 3 h in 4 mL of Hanks salt buffer (GIBCO) at 37 °C under an atmosphere of 95% air and 5% CO_2. The buffer contained 5 or 50 mM glucose and 0–10^{-5} M of test compound. At the end of the incubation period sorbitol levels were determined by a spectrofluorometric enzymatic assay.[19]

The inhibition of aldose reductase in vivo was assessed in rats that were fed 20% galactose for 4 days. The test compounds were administered in the diet. At the termination of the experiment, the galactitol levels were determined in trichloroacetic acid extracts of the lenses and sciatic nerves by a modification of the method of Kraml and Cosyns.[20b] The galactitol levels in the drug-treated galactosemic animals were compared to that in the galactosemic control animals by Dunnett's multiple comparison.

Acknowledgment. We gratefully acknowledge the assistance and suggestions of Dr. Alan H. Katz, Nancie Senko, and Kimberly Conway of the Molecular Modeling Group in obtaining the stereoviews shown in Figures 1–6. We are also thankful to Karen Muldoon for her molecular modeling contributions early in the project.

Registry No. 8, 88245-15-2; 9, 118896-19-8; 10, 118896-20-1; (*E*)-11, 118896-18-7; (*Z*)-11, 118896-21-2; (*E*)-12, 118896-17-6; (*Z*)-12, 118896-22-3; 14, 118896-24-5; 15, 118896-25-6; 16, 81-84-5; 17, 5472-84-4; 18, 118896-26-7; 19, 118896-27-8; 20, 20494-87-5; 21, 93015-68-0; 22, 118896-28-9; 23, 118896-29-0; 24, 118896-30-3; 25, 118896-31-4; 26, 118896-32-5; $CH_2(CO_2Et)_2$, 105-53-3; 1-naphthaldehyde, 66-77-3; ethyl propionate, 105-37-3; dimethyl malonate, 108-59-8; carbon tetrabromide, 558-13-4; methyl [6-methoxy-5-(trifluoromethyl)-1-naphthalenyl]propanoate, 118896-23-4; aldose reductase, 9028-31-3.

Supplementary Material Available: Cartesian coordinates and corresponding energies for computed low-energy conformations of sorbinil, tolrestat, ICI-105,552, and hybrid compound 7 (11 pages). Ordering information is given on any current masthead page.

Topography and Conformational Preferences of 6,7,8,9-Tetrahydro-1-hydroxy-*N*,*N*-dipropyl-5*H*-benzocycloheptene-6-ylamine. A Rationale for the Dopaminergic Inactivity

Anders Karlén,† Anne Helander,‡ Lennart Kenne,§ and Uli Hacksell*,†

Department of Organic Pharmaceutical Chemistry, Uppsala Biomedical Center, University of Uppsala, Box 574, S-751 23 Uppsala, Sweden, Analytical Chemistry, R & D, KabiVitrum AB, S-112 87 Stockholm, Sweden, and Department of Organic Chemistry, Arrhenius Laboratory, University of Stockholm, S-106 91 Stockholm, Sweden. *Received July 5, 1988*

In an attempt to rationalize the inability of phenolic benzocycloheptenylamines to activate dopamine (DA) D_2 receptors, we have studied the conformational preferences and topography of 6,7,8,9-tetrahydro-1-hydroxy-*N*,*N*-dipropyl-5*H*-benzocycloheptene-6-ylamine (1). Preferred conformations of 1 have been defined by use of experimental (NMR spectroscopic studies) and theoretical (MMP2, AM1, and MNDO calculations) methods. Topographical characteristics were studied by use of molecular graphics. Results from the MMP2 calculations agree with those from the AM1 calculations and the NMR spectroscopic study—1 seems to preferentially adopt chair conformations with a pseudoequatorial C6 substituent. The MNDO calculations, however, produced results that deviate considerably from those of the other theoretical methods. Most likely, pharmacophore conformations of (*S*)-1 do not present volumes that are part of the DA D_2 receptor essential volume. Therefore, it appears that the energy penalty paid by the pharmacophore conformations is responsible for the dopaminergic inactivity of (*S*)-1. The inactivity of (*R*)-1 may be due to high energies of pharmacophore conformations and/or to steric factors since these conformations produce large excess volumes that may be part of the DA D_2 receptor essential volume. The model used in the present report—a flexible pharmacophore combined with a partial receptor-excluded volume—might be used in the design of new DA D_2 receptor agonists.

Computer-aided drug design (CADD) has developed into a powerful technique for the medicinal chemist of today.[1] Based on knowledge of enzyme structures[2] or on deduced receptor (enzyme) excluded volumes,[3] computer graphics can be used to design drugs. However, when it comes to flexible molecules, one does not know what energy criteria to use when defining biologically relevant conformations. If, e.g., the energies of all potential stabilizing interactions in a drug–receptor complex are added, the sum frequently is larger than 10 kcal/mol, even for rather small molecules.[4] This would indicate that conformations with fairly high energies might be of biological relevance. On the other hand, it has been argued that conformational energy penalties as small as 3–4 kcal/mol lead to biological inactivity.[1e,5] Clearly, this poses a dilemma for medicinal chemists working with CADD.

We and others have previously defined a dopamine (DA) D_2 receptor agonist pharmacophore[6] and a partial DA D_2

† University of Uppsala.
‡ KabiVitrum AB.
§ University of Stockholm.

(1) (a) Hopfinger, A. J. *J. Med. Chem.* **1985**, *28*, 1133–1139. (b) Frühbeis, H.; Klein, R.; Wallmeier, H. *Angew. Chem., Int. Ed. Engl.* **1987**, *26*, 403–418. (c) Sheridan, R. P.; Venkataraghavan, R. *Acc. Chem. Res.* **1987**, *20*, 322–329. (d) Marshall, G. R. *Annu. Rev. Pharmacol. Toxicol.* **1987**, *27*, 193–213. (e) Tollenaere, J. P.; Janssen, P. A. J. *Med. Res. Rev.* **1988**, *8*, 1–25.
(2) (a) Hol, W. G. J. *Angew. Chem., Int. Ed. Engl.* **1986**, *25*, 767–778. (b) Hansch, C.; Klein, T. E. *Acc. Chem. Res.* **1986**, *19*, 392–400.
(3) (a) Sufrin, J. R.; Dunn, D. A.; Marshall, G. R. *Mol. Pharmacol.* **1981**, *19*, 307–313. (b) Klunk, W. E.; Kalkman, B. L.; Ferrendelli, J. A.; Covey, D. F. *Mol. Pharmacol.* **1983**, *23*, 511–518.
(4) (a) Andrews, P. R.; Craik, D. J.; Martin, J. L. *J. Med. Chem.* **1984**, *27*, 1648–1657. (b) Andrews, P. *Trends Pharmacol. Sci.* **1986**, 148–151.
(5) Pettersson, I.; Liljefors, T. *J. Comput.-Aided Mol. Des.* **1987**, *1*, 143–152.

0022-2623/89/1832-0765$01.50/0

Table I. Geometrical Parameters for Low-Energy (MMP2) Conformations of (S)-1[a]

conf	τ_N,[b] deg	τ_1,[c] deg	τ_2,[d] deg	τ_A,[e] deg	τ_B,[f] deg	$\tau_{A'}$,[g] deg	$\tau_{B'}$,[h] deg	rel steric energy, kcal/mol
I	179	-111	-84	-48	-171	176	-171	0.2
II	178	-110	-84	-52	-57	175	-170	0.6
III	179	-111	-84	-49	-170	173	-56	0.5
IV	178	-110	-84	-54	-56	171	-54	0.7
V	-171	-110	-86	-54	-172	-66	-174	2.4
VI	-51	-111	-82	-168	54	51	170	0.2
VII	-52	-111	-82	-169	170	50	170	0[i]
VIII	-50	-111	-83	-168	170	53	56	0.3
IX	-50	-111	-83	-166	53	55	55	0.2
X	-38	-112	-83	-59	-167	60	50	2.5
XI	54	115	82	65	-178	176	-169	0.5
XII	54	114	82	64	-177	174	-56	0.4
XIII	58	116	82	-178	57	-67	180	1.1
XIV	58	116	82	179	171	-66	-179	1.0

[a] Only conformations with τ(C9a,C1,O,H) ≈ 180° are included and conformations with energies larger than 2.5 kcal/mol above the global minimum have been omitted. [b] τ_N = τ(C5,C6,N,electron pair). [c] τ_1 = τ(C4,C4a,C5,C6). [d] τ_2 = τ(C4a,C5,C6,C7). [e] τ_A = τ(C6,N,Cα,Cβ). [f] τ_B = τ(N,Cα,Cβ,Cγ). [g] $\tau_{A'}$ = τ(C6,N,Cα',Cβ'). [h] $\tau_{B'}$ = (N,Cα',Cβ',Cγ'). [i] Steric energy = 18.5 kcal/mol.

Table II. Geometrical Parameters for Low-Energy (MMP2, AM1, and MNDO) Conformations of (S)-2

		MMP2				AM1				MNDO			
conf	ring conf[a]	τ_N[b]	τ_1[b]	τ_2[b]	ΔE	τ_N[b,c]	τ_1[b]	τ_2[b]	ΔH_f	τ_N[b,c]	τ_1[b]	τ_2[b]	ΔH_f
I	A	45	-107	-83	2.0	47	-107	-83	3.2	30	-112	-81	3.3
II	A	174	-111	-83	0.3	173	-112	-85	0[e]	167	-113	-81	0.3
III	A	-51	-111	-82	0[d]	-50	-110	-84	0[e]	-40	-115	-80	0[f]
IV	B	56	115	82	0.1	55	115	83	3.7	51	117	80	6.2
V	B	-165	113	73	3.8	-167	112	75	3.6	-176	115	71	4.1
VI	B	-34	112	74	4.3	-31	113	74	3.8	-15	117	69	3.2
VII	C	59	140	89	3.8	61	140	86	7.2	58	144	82	9.4
VIII	C	176	117	48	4.9	174	115	48	6.4	169	116	49	4.9
IX	C	-54	121	48	4.3	-52	119	47	4.1	-46	123	47	5.7
X	D	50	-136	-90	3.8	48	-137	-91	4.6	44	-138	-88	8.1
XI	D	171	-141	-86	3.9	168	-140	-88	2.5	159	-138	-85	3.8
XII	D	-56	-143	-84	2.8	-54	-142	-86	2.3	-42	-150	-80	4.1
XIII	E	58	99	50	3.6	58	102	48	6.0	55	104	47	8.4
XIV	E	176	115	18	2.9	176	116	19	3.6	167	117	20	3.2
XV	E	-46	117	18	2.7	-45	117	19	3.2	-29	120	19	2.5
XVI	F	60	-113	-21	2.5	59	-115	-22	5.3	57	-113	-21	8.3
XVII	F	-169	-109	-32	4.5	-172	-109	-34	4.6	-179	-108	-33	4.8
XVIII	F	-40	-108	-33	4.9	-39	-109	-35	4.3	-28	-110	-32	3.6

[a] Defined in Figure 2. [b] Defined in footnote in Table I. [c] An N-electron pair was added to the AM1 and MNDO geometries (using MIMIC) to permit calculation of the τ_N values. [d] Steric energy = 13.1 kcal/mol. [e] Heat of formation = -32.9 kcal/mol. [f] Heat of formation = -23.4 kcal/mol.

receptor excluded volume.[7] This volume is composed of four stereoselective and potent DA D_2 receptor agonists[8] in pharmacophore conformations.[7] Interestingly, the *S* enantiomer of the DA D_2 receptor inactive 6,7,8,9-tetrahydro-1-hydroxy-*N*,*N*-dipropyl-5*H*-benzocyclohepten-6-ylamine (1),[9,10] is able to assume DA D_2 pharmacophore

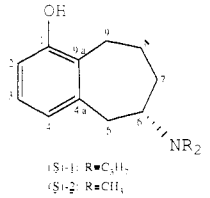

(S)-1: R=C_3H_7
(S)-2: R=CH_3

conformations, and these conformations present only minor excess volumes when fitted into the partial receptor-excluded volume (Figure 1; vide infra). In the present investigation we have therefore defined minimum-energy conformations and energies of pharmacophore conformations of 1 by use of theoretical and experimental methods. The results indicate that the inactivity of (S)-1 is due to the large energy penalty of pharmacophore conformations.

Methods

The synthesis of 1 has been previously reported.[9] The structural modelling was performed by use of the interactive computer graphics program MIMIC[11] (Methods for

(6) (a) Johansson, A. M.; Karlén, A.; Grol, C. J.; Sundell, S.; Kenne, L.; Hacksell, U. *Mol. Pharmacol.* **1986**, *30*, 258–269. (b) Froimowitz, M.; Neumeyer, J. L.; Baldessarini, R. J. *J. Med. Chem.* **1986**, *29*, 1570–1573. (c) Liljefors, T.; Wikström, H. *J. Med. Chem.* **1986**, *29*, 1896–1904.
(7) Johansson, A. M.; Nilsson, J. L. G.; Karlén, A.; Hacksell, U.; Svensson, K.; Carlsson, A.; Kenne, L.; Sundell, S. *J. Med. Chem.* **1987**, *30*, 1135–1144.
(8) For recent reviews on DA-receptor agonists, see, for example: Kaiser, C.; Jain, T. *Med. Res. Rev.* **1985**, *5*, 145–229. Cannon, J. G. *Prog. Drug Res.* **1985**, *29*, 303–414.
(9) Hacksell, U.; Arvidsson, L.-E.; Svensson, U.; Nilsson, J. L. G.; Wikström, H.; Lindberg, P.; Sanchez, D.; Hjorth, S.; Carlsson, A.; Paalzow, L. *J. Med. Chem.* **1981**, *24*, 429–434.
(10) The 1,3-dihydroxy analogue of 1 have also been found to lack DA receptor active properties: Cannon, J. G.; Pease, J. P.; Hamer, R. L.; Ilhan, M.; Bhatnagar, R. K.; Long, J. P. *J. Med. Chem.* **1984**, *27*, 186–189. Several studies of nonhydroxylated 6-aminobenzocycloheptenylamine derivatives have also appeared in the literature. See: Rusterholz, D. B.; Long, J. P.; Flynn, J. R.; Cannon, J. G.; Lee, T.; Pease, J. P.; Clemens, J. A.; Wong, D. T.; Bymaster, F. P. *Eur. J. Pharmacol.* **1979**, *55*, 73–82. Cannon, J. G.; Perez, J. A., Pease, J. P.; Long, J. P.; Flynn, J. R.; Rusterholz, D. B.; Dryer, S. E. *J. Med. Chem.* **1980**, *23*, 745–749.
(11) Liljefors, T. *J. Mol. Graphics* **1983**, *1*, 111–117.

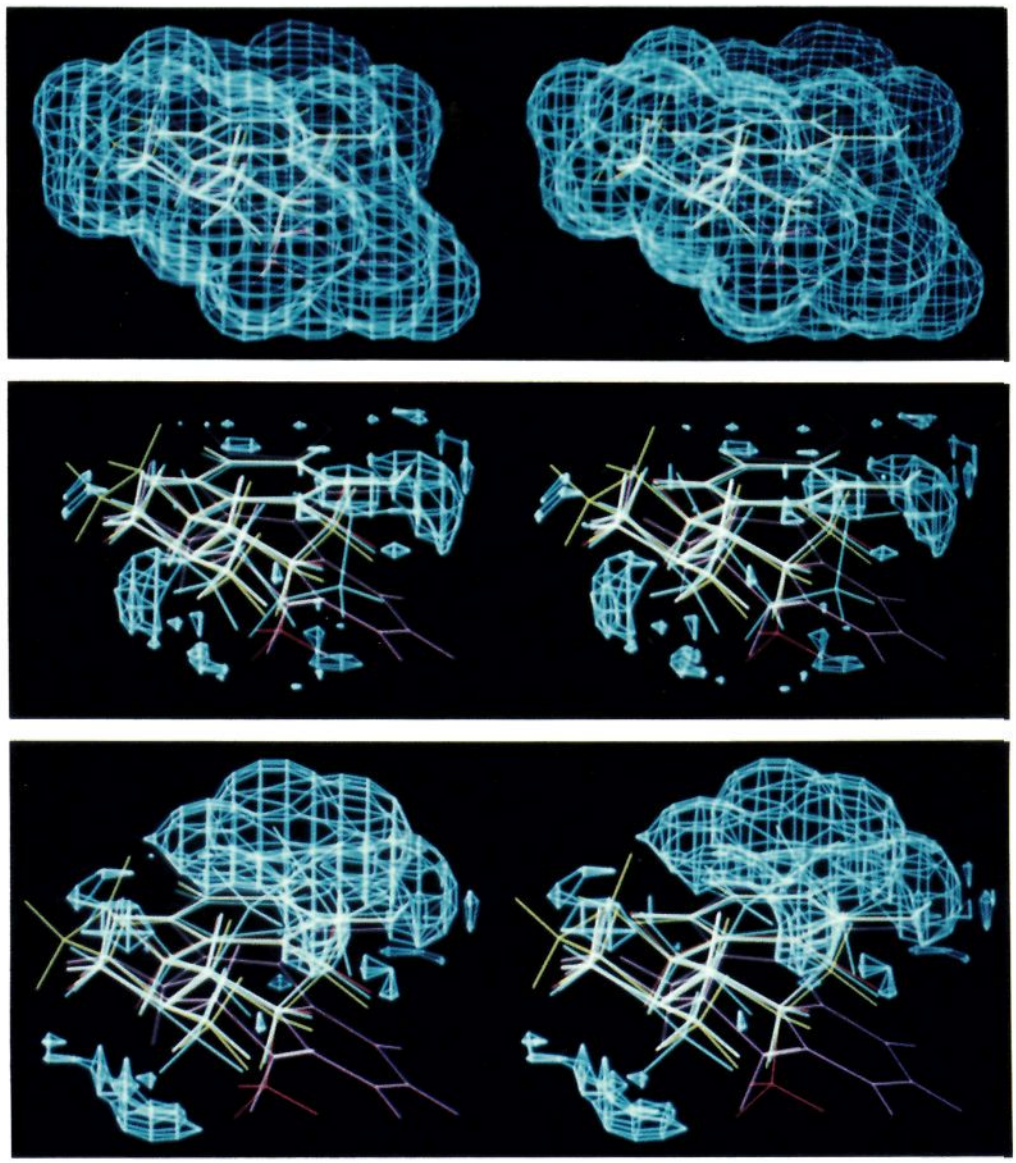

Figure 1. Excess volumes produced by the van der Waals volumes of pharmacophore conformations of (*S*)-**2** (middle) and (*R*)-**2** (bottom) when compared with the previously defined partial DA D_2 receptor excluded volume (top).[7] The appropriate conformations of (*S*)-**2** and (*R*)-**2** were identified as those giving the best fit to the pharmacophore conformation of the *N*,*N*-dimethylamino derivative of (*S*)-5-OH-DPAT (conformation A in ref 23). Conformations were generated by using the torsion angle driver routine in the MMP2 program (Figure 7d and ref 32). To obtain a consistent alignment of the molecules in space, the *N*,*N*-dimethylamino derivative of (2*S*)-5-OH-DPAT was used as a template in the least square fitting procedure—the hydroxyl group, N, N-electron pair, C7, and C8a were fitted with the corresponding structural elements of (*S*)-**2** and (*R*)-**2**. The average distance between fitted atoms was 0.23 and 0.17 Å, respectively. To generate the excess volume representations of (*S*)-**2** and (*R*)-**2**, the MVOLUME command of SYBYL was used. The union of the volumes of the four molecules comprising the partial DA D_2 receptor excluded volume was subtracted from the union of the combined volumes of these four molecules and (*S*)-**2** or (*R*)-**2**, respectively. Color code: (2*S*)-5-hydroxy-2-(*N*,*N*-dimethylamino)tetralin (white), (2*R*,3*S*)-5-hydroxy-3-methyl-2-(*N*,*N*-dimethylamino)tetralin (red), (4a*S*,10b*S*)-7-hydroxy-4-methyl-1,2,3,4a,5,6,10b-octahydrobenzo[*f*]quinoline (yellow), (*R*)-apomorphine (purple), (*R*)- and (*S*)-**2** (light blue).

Interactive Modelling In Chemistry), Chem-X,[12] and SYBYL (Figure 1). MMP2 calculations were performed with Allingers MMP2 1980-force field[13] to which had been added parameters for the phenol[14] and amino groups.[15] AM1[16] and MNDO[17] calculations were carried out on the free bases with the standard procedure, as implemented in the AMPAC program.[18] Geometries in Tables I and II were obtained without restrictions in the minimization process. To optimize the geometry of the conformations more ac-

(12) Chem-X, developed and distributed by Chemical Design Ltd, Oxford, England.
(13) (a) Allinger, N. L. *J. Am. Chem. Soc.* **1977**, *99*, 8127–8134. (The MMP2 program is available from the Quantum Chemistry Program Exchange, University of Indiana, Bloomington, IN 47405 and from Molecular Design Ltd., 2132 Farallon Drive, San Leandro, CA 94577.)
(14) Dodziuk, H.; von Voithenberg, H.; Allinger, N. L. *Tetrahedron* **1982**, *38*, 2811–2819.
(15) Profeta, S., Jr.; Allinger, N. L. *J. Am. Chem. Soc.* **1985**, *107*, 1907–1918.
(16) Dewar, M. J. S.; Zoebisch, E. G.; Healy, E. F.; Stewart, J. J. P. *J. Am. Chem. Soc.* **1985**, *107*, 3902–3909.
(17) Dewar, M. J. S.; Thiel, W. *J. Am. Chem. Soc.* **1977**, *99*, 4899–4907, 4907–4917.
(18) Available from the Quantum Chemistry Program Exchange (QCPE). Program No. 506.

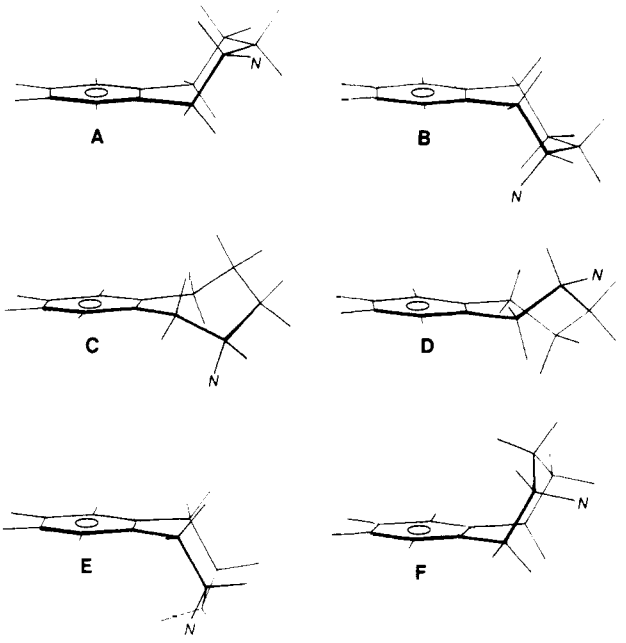

Figure 2. Energy-minimized (MMP2) benzocycloheptene conformations having C_s (conformations A, B, E, and F) or C_2 symmetry (conformations C and D). The orientation of a *S* C6-substituent (pseudoequatorial or pseudoaxial) is indicated by the letter N.

curately when the torsion angle τ_3 was driven (Figure 9), the keyword "PRECISE" was used. This keyword reduces the tolerance for all electronic and geometrical changes by a factor of 100. When geometries are defined by internal coordinates such as torsion angles or bond angles (AM1 and MNDO), calculations may be abandoned since small changes in internal coordinates may cause a large change in the distance between covalently bound atoms. To eliminate this problem the keyword "XYZ" was used. In this mode the program uses Cartesian coordinates to optimize molecular geometries.

Calculations were done on a Microvax II computer. Computational times ranged from 1 to 25 min, 2 to 5 h, and 5 to 15 h per minimization for MMP2, AM1, and MNDO, respectively, and 12 days (both directions) for the torsion angle driver experiment (AM1).

^1H and ^{13}C NMR spectra were recorded on a JEOL GX-400 spectrometer using 0.05 M solutions of 1·HBr at 40 °C. Chemical shifts were measured relative to internal tetramethylsilane. Apparent coupling constants were calculated from expanded spectra (2 Hz/cm) and refined by use of the spin simulation program INMGX-COMIC-2, available in the GX software. Standard pulse sequences were used for the two-dimensional experiments with 45° or 90° mixing pulses. The NOE difference experiment was performed with 1.5 s preirradiation at δ 6.72 ppm. A total of 800 accumulations were used with cycles of eight accumulations for on and off resonances, respectively, with a 10-s delay for relaxation between the pulses.

Definition of Conformational Parameters of 1

Conformational studies of benzocycloheptene using ^1H NMR spectroscopy[19] and calculative methods[20] have indicated that the cycloheptene ring prefers the chair (C_s symmetry) over the twist (C_2 symmetry) and boat (C_s symmetry) conformations. When a 6-amino substituent is introduced in the benzocycloheptene ring system, six potential low-energy conformations (two chair, two twist, and two boat conformations) may form (Figure 2). That 1 can adopt a large number of low-energy conformations is indicated further by the mobility of the two *N*-propyl groups, and by the possibility of rotation around the C1–O and C6–N bonds. To describe the geometry of 1, seven parameters are needed. The torsion angle $\tau_N = \tau$(C5, C6, N, H, or electron pair) defines the direction of the N–H bond (N-electron pair). The torsion angles $\tau_1 = \tau$(C4,C4a,C5,C6) and $\tau_2 = \tau$(C4a,C5,C6,C7) describe the conformation of the cycloheptene ring. The torsion angles $\tau_A = \tau$(C6,N,Cα,Cβ) and $\tau_B = \tau$(N,Cα,Cβ,Cγ) define the conformation of the *N*-propyl group, which in a clockwise sense is next to the N–H bond (N-electron pair) when viewing along the C6–N bond. Similarly, the conformation of the second *N*-propyl group is defined by $\tau_A' = \tau$(C6,N,Cα',Cβ') and $\tau_B' = \tau$(N,Cα',Cβ',Cγ').[21]

Determination of Conformational Preferences of (*S*)-1

MMP2 Calculations. The calculations were performed on the free bases although DA agonists probably interact with the receptor(s) in the protonated form.[22]

To map the conformational space of (*S*)-1 we adopted a strategy that is similar to that used previously[23] for the conformational analysis of a large series of 2-(*N*,*N*-dipropylamino)tetralins. On the basis of the successful use of this strategy, we are confident that this approach makes it possible to detect significantly populated conformations. Thus, a 6-*N*,*N*-dimethylamino substituent was added in three different ways, to each of the six conformations in Figure 2, so that τ_N = 60°, 180°, and −60°. The starting geometry of the hydroxyl group was always set at τ(C9a, C1, O, H) = 180°.[24] The resulting 18 "starting geometries" were minimized and conformations with energies > 2.9 kcal/mol[25] above the global minimum were discarded. To each of the remaining conformations were added two methyl groups so that the nine possible staggered "6-(*N*,*N*-diethylamino)benzocycloheptene geometries" were formed from each "6-(*N*,*N*-dimethylamino)benzocycloheptene" conformation. These new starting geometries were minimized and conformations with energies > 2.7 kcal/mol[25] above the global minimum were discarded. In the final minimization of the "6-(*N*,*N*-dipropylamino)-benzocycloheptene geometries", all staggered *N*,*N*-dipropylamino rotamers were minimized. By use of this approach we have identified 14 low-energy conformations (within 2.5 kcal/mol of the global minimum)[25] of (*S*)-1. These are chair conformations with pseudoequatorial (conformations I–X) or pseudoaxial (conformations XI–

(19) (a) von Kabuss, S.; Friebolin, H.; Schmid, H. *Tetrahedron Lett.* **1965**, *9*, 469–472. (b) Kabuss, S.; Schmid, H. G.; Friebolin, H.; Faisst, W. *Org. Magn. Reson.* **1969**, *1*, 451–465. (c) St-Jacques, M.; Vaziri, C. *Org. Magn. Reson.* **1972**, *4*, 77–93.

(20) (a) Tochtermann, W. *Fortsch. Chem. Forsch.* **1970**, *15*, 378–444. (b) Kabuss, S.; Schmid, H. G.; Friebolin, H.; Faisst, W. *Org. Magn. Reson.* **1970**, *2*, 19–41. (c) Favini, G.; Nava, A. *Gazz. Chim. Ital.* **1974**, *104*, 621–624.

(21) For definitions of torsion angle and related concepts, see: Klyne, W.; Prelog, V.; *Experientia* **1960**, *16*, 521–523.

(22) See, for example: Seeman, P.; Guan, H.-C. *Mol. Pharmacol.* **1987**, *32*, 760–763. Andersson, K.; Kuruvilla, A.; Uretsky, N.; Miller, D. D. *J. Med. Chem.* **1981**, *24*, 683–687. Chang, Y.-A.; Ares, J.; Andersson, K.; Sabol, B.; Wallace, R. A.; Farooqui, T.; Uretsky, N.; Miller, D. D. *J. Med. Chem.* **1987**, *30*, 214–218.

(23) Karlén, A.; Johansson, A. M.; Kenne, L.; Arvidsson, L.-E.; Hacksell, U. *J. Med. Chem.* **1986**, *29*, 917–924.

(24) Test calculations demonstrate that conformations having τ(C9a,C1,O,OH) = 180° are about 0.2–0.7 kcal/mol higher in energy.

(25) The cut-off values 2.9, 2.7, and 2.5 kcal/mol were choosen to make it possible to identify conformations of (*S*)-1 that are significantly (>1–2%) populated according to a Boltzman distribution at 37 °C.

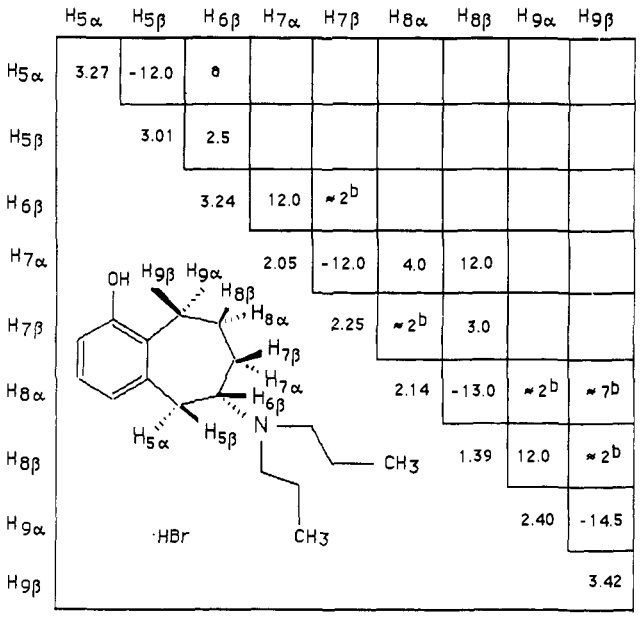

Figure 3. Selected ^{1}H NMR spectroscopic data of 1·HBr in CD_3OD at 25 °C. Chemical shifts (in ppm) are shown on the diagonal. Proton–proton coupling constants are in hertz. (a) Not determined due to overlapping signals. (b) The value is approximate due to the complex splitting pattern.

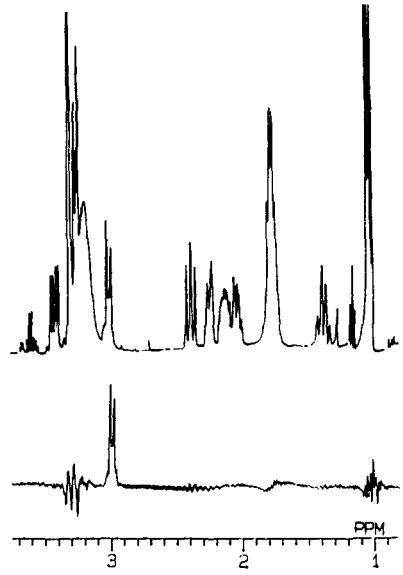

Figure 4. NOE difference spectrum (bottom) of the aliphatic region of the 400-MHz ^{1}H NMR spectrum of 1·HBr in CD_3OD (top) obtained by irradiation of H4 (δ 6.72 ppm).

XIV) *N,N*-dipropylamino groups (Table I).[26]

AM1 and MNDO Calculations. In these calculations, (*S*)-6,7,8,9-tetrahydro-1-hydroxy-*N,N*-dimethyl-5*H*-benzocyclohepten-6-ylamine, (*S*)-**2**, was used as a model for (*S*)-**1**. The 18 low-energy geometries of (*S*)-**2**, obtained from the MMP2 calculations (vide supra), were minimized by using semiempirical (AM1 and MNDO) calculations. The results are depicted in Table II in which also results from the MMP2 calculations are included for comparison. It is noteworthy that, although the methods used are based on completely different assumptions,[27] they predict the same lowest energy conformation. The minor deviation in geometries obtained by MMP2 and AM1 is impressive; e.g., the largest difference observed in τ_N, τ_1, or τ_2 is 3° (Table II). In addition, the MMP2 and AM1 calculations give similar trends in relative energies. However, the AM1 calculations consistently assign higher relative energies to conformations having τ_N values around 60° than does MMP2. Thus, according to MMP2, conformation IV (having τ_N around 55°) is close in energy (0.1 kcal/mol) to the minimum-energy conformation whereas AM1 predicts it to be 3.7 kcal/mol above the global energy minimum.

The MNDO calculations resulted in geometries (torsion angles) that differ considerably from those produced by MMP2 and AM1; e.g., the τ_N value of conformation I differs from that of the corresponding AM1 and MMP2 conformations with 17° and 15°, respectively. In addition, the relative energies prediced by MNDO are frequently considerably larger than those obtained with the other two methods. Given the successful use of MMP2 calculations to predict relative energies and geometries of phenolic 2-aminotetralins,[28] it is likely that the MMP2 and AM1 calculations give better results than MNDO in these and similar systems.

NMR Spectroscopy. High-resolution ^{1}H NMR spectral data for 1·HBr in CD_3OD are shown in Figure 3. Use of 400-MHz spectroscopy allowed analysis of several resonances by first-order approximations although some signals were complicated due to higher order couplings or overlapping resonances. However, C–H correlation, COSY, and spin–spin decoupling experiments allowed assignments of the signals and spin–spin simulations verified the obtained coupling constants. The assignment of the pseudoequatorial $H_{5\beta}$ proton was verified by an NOE difference experiment in which preirradiation of the aromatic C4-H induced a significant enhancement of the signal at δ 3.01 ppm (Figure 4). The presence of the large coupling constants $J_{7\alpha,8\beta}$ and $J_{8\beta,9\alpha}$ as well as the 7 Hz coupling constant $J_{8\alpha,9\beta}$ agree with a predominance of a chair conformation of 1·HBr in CD_3OD; an anti relationship between $H_{7\alpha}$, $H_{8\beta}$, and $H_{9\alpha}$ is indicated and the angle between $H_{8\alpha}$ and $H_{9\beta}$ seems to be smaller than 60°. The large coupling constant $J_{6\beta,7\alpha}$ suggests that the *N,N*-dipropylammonium group assumes a pseudoequatorial disposition. The coupling constant $J_{5\alpha,6\beta}$ was not obtained due to the complexity of the signals which depended on the small difference in resonance frequencies for these protons. The signal for $H_{6\beta}$ appears at higher field than the corresponding proton

(26) Estimation of a Boltzman distribution (at 37 °C) based on the steric energies (Table I) indicates that 1 prefers to assume a chair conformation with a pseudoequatorial *N,N*-dipropylamino group (79%). The population of chair conformers with a pseudoaxial *N,N*-dipropylamino substituent was estimated to 21%.

(27) In molecular mechanics, the atoms and their associated electrons are treated as units interconnected by potential functions that describe structural features like bond lengths and bond angles. In contrast, in semiempirical methods (e.g. AM1 and MNDO) the molecules are described by combining different sets of atomic orbitals to molecular orbitals. The combinations of these orbitals, that give the lowest electronic energy, are then determined. See, for example: Burkert, U.; Allinger, N. L. *Molecular Mechanics*; American Chemical Society: Washington, DC, 1982. Clark, T. *A Handbook of Computational Chemistry*; Wiley: New York, 1985.

(28) There is good agreement between experimental (^{1}H NMR spectroscopy and X-ray crystallography) and theoretical (MMP2) results; see ref 6a, 7, 23, and the following: (a) Johansson, A. M.; Nilsson, J. L. G.; Karlén, A.; Hacksell, U.; Sanchez, D.; Svensson, K.; Hjorth, S.; Carlsson, A.; Sundell, S.; Kenne, L. *J. Med. Chem.* **1987**, *30*, 1827–1837. (b) Arvidsson, L.-E.; Karlén, A.; Kenne, L.; Norinder, U.; Sundell, S.; Hacksell, U. *J. Med. Chem.* **1988**, *30*, 212–221. (c) Mellin, C.; Björk, L.; Karlén, A.; Johansson, A. M.; Andén, N. E.; Hacksell, U. *J. Med. Chem.* **1988**, *31*, 1130–1140.

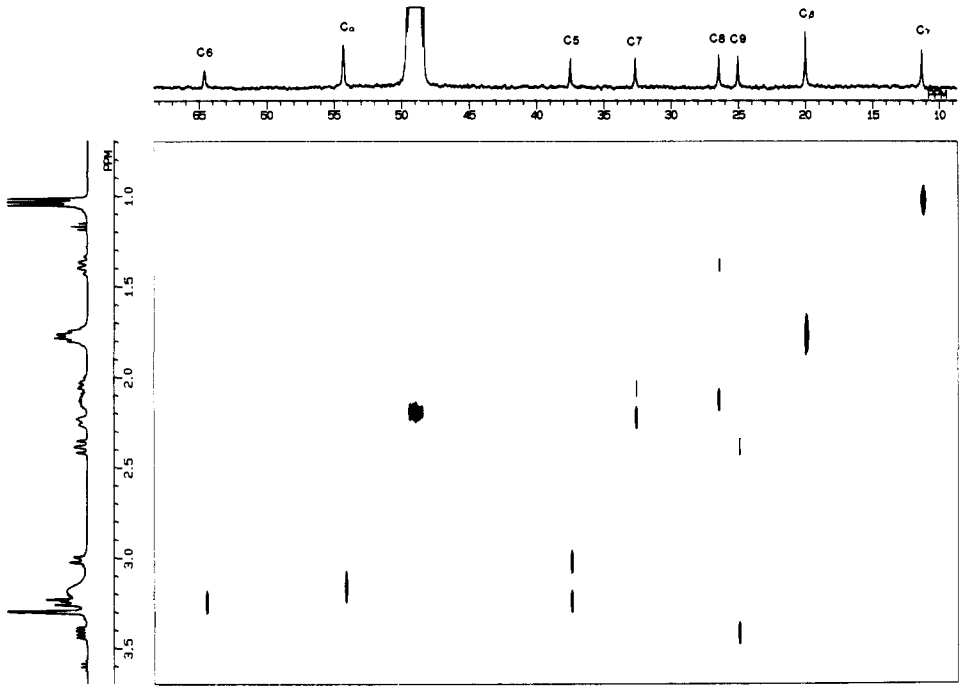

Figure 5. Partial ^{13}C–^{1}H NMR chemical shift correlation spectrum (aliphatic region) of 1·HBr in CD_3OD. The triplet at 1.17 ppm and the quartet at 3.59 ppm are due to diethyl ether.

(C2-H) of 5-hydroxy-2-(dipropylamino)tetralin (5-OH-DPAT),[23] indicating that the former proton is shielded by the aromatic ring current. Shielding of this proton as well as the shielding observed of $H_{8\beta}$ is likely to occur when 1·HBr adopts conformation A (Figure 2). The ^{13}C NMR spectrum of 1 was also recorded, and the signals were assigned by use of 2D chemical shift correlation spectroscopy (Figure 5).

Taken together, the ^{1}H NMR data indicate that conformations such as I–X are favored in solution and not those that are similar to XI–XIV (Table I). Thus, both experimental (^{1}H NMR spectroscopy) and theoretical (MMP2, AM1, MNDO) data suggest that a chair conformation of 1 with a pseudoequatorial *N,N*-dipropylamino (ammonium) substituent is energetically favored.

Definition of Pharmacophore Conformations of (*S*)-1

Receptors are dynamic entities. Thus, a pharmacophore should have some flexibility. Three key intramolecular distances for DA-receptor agonists have been defined previously;[29] the distance from the center of the aromatic ring to the nitrogen (N–ArC distance), the distance from the plane of the aromatic ring to the nitrogen (N–ArP distance), and the distance from a "meta" hydroxyl oxygen to the nitrogen (N–O distance). It has also been observed that the relative orientation of the N-electron pair (or N^+–H bond) is of critical importance for DA D_2 receptor activation.[30] However, it is not known how far the DA D_2 pharmacophore can deviate from that in, e.g., (6*R*)-apomorphine (N–ArP = 1.2 Å, N–ArC = 5.1 Å, N–O = 6.5 Å) or (2*S*)-5-OH-DPAT (N–ArP = 0.03 Å, N–ArC = 5.2 Å, N–O = 6.6 Å). In the present investigation, we chose to treat conformations of the model compound (*S*)-2 with N–ArP distances within 0.50 ± 0.75 Å and τ_N values around 80° as pharmacophore conformations.

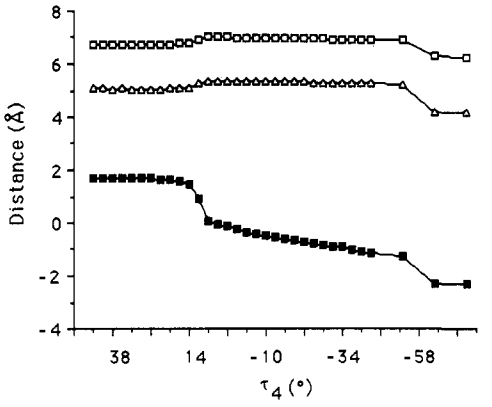

Figure 6. Plot illustrating the relationship between τ_4 and key intramolecular distances in (*S*)-1. N–O (□): distance from a "meta" hydroxyl oxygen to the nitrogen atom. N–ArP (■): distance from the plane of the aromatic ring to the nitrogen atom. N–ArC (△): distance from the center of the aromatic ring to the nitrogen atom. Distances were measured from geometries obtained by driving the torsion angle τ_4 (Figure 7d). Positive values denote that the nitrogen atom is situated above the aromatic ring (compare conformation A, Figure 2). Dummy atoms were used to define the plane and the center of the aromatic ring.

Estimation of Energies of Pharmacophore Conformations of (*S*)-2

The torsion angle driver method[31] was used to obtain energies and acceptable geometries of pharmacophore

(29) For discussions on important intramolecular distances in DA-receptor agonists, see, for example, ref 9 and Seeman, P. *Pharmacol. Rev.* **1980**, *32*, 229–313.

(30) See, e.g., ref 5, 6a–c, 7, 28b, and the following: Tedesco, J. L.; Seeman, P.; McDermed, J. D. *Mol. Pharmacol.* **1979**, *16*, 369–381. Seeman, P.; Watanabe, M.; Grigoriadis, P.; Tedesco, J. L.; George, S. R.; Svensson, U.; Nilsson, J. L. G.; Neumeyer, J. L. *Mol. Pharmacol.* **1985**, *28*, 391–399. Wilkström, H.; Lii, J.-H.; Allinger, N. L. *J. Med. Chem.* **1987**, *30*, 1115–1120.

(31) Wiberg, K. B.; Boyd, R. H. *J. Am. Chem. Soc.* **1972**, *94*, 8426–8430. For a discussion of problems related to the torsion angle driver method, see: Müller, K. *Angew. Chem., Int. Ed. Engl.* **1980**, *19*, 1–78. Burkert, U.; Allinger, N. L. *J. Comput. Chem.* **1982**, *3*, 40–46.

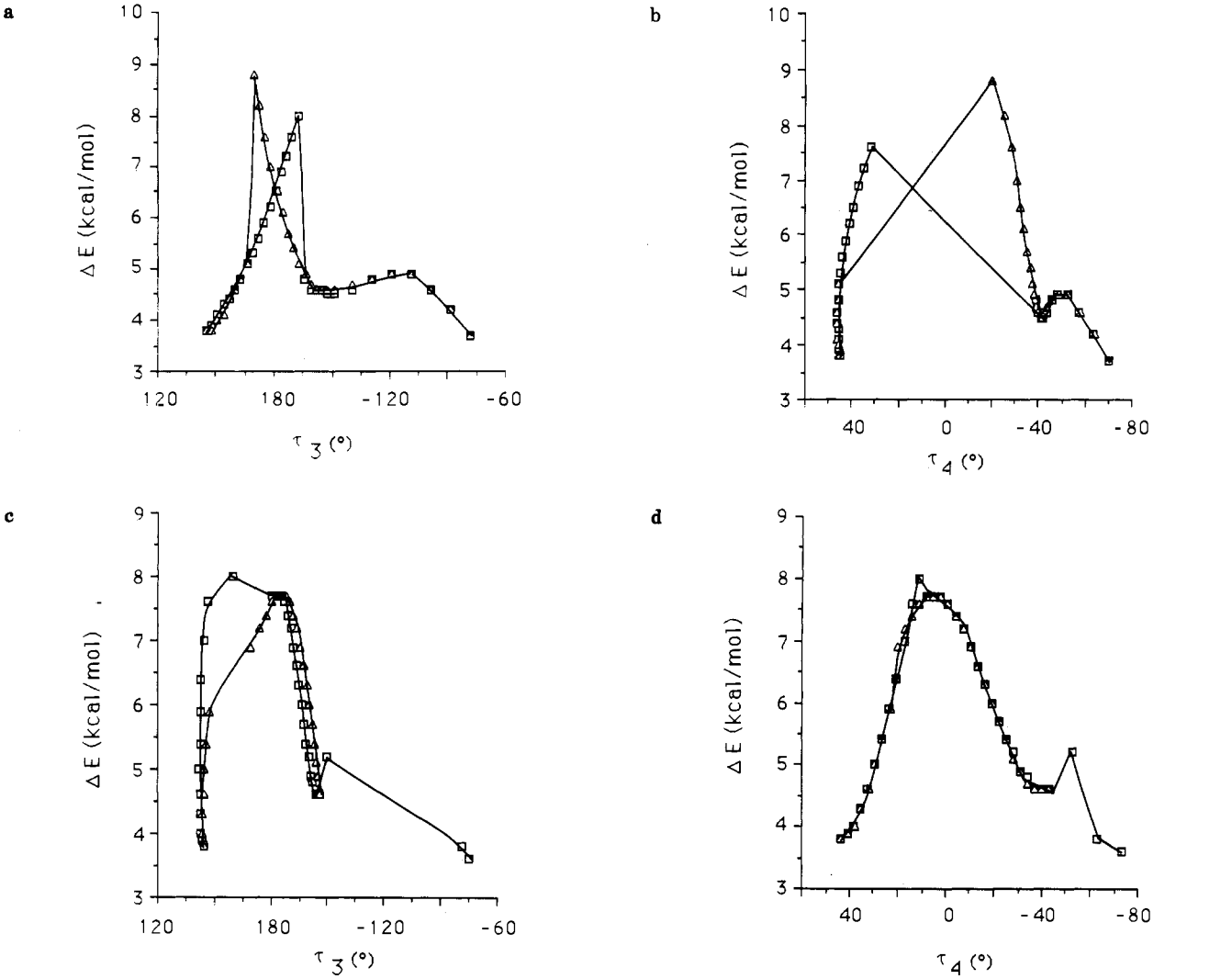

Figure 7. Plot of relative steric energies (MMP2) obtained when driving τ_3 (a) and τ_4 (d) of (*S*)-**2**, between the twist and boat conformations. In addition, the concomitant changes in τ_4 when τ_3 was used as the reaction coordinate (b) and in τ_3 when τ_4 was used as the reaction coordinate (c) are shown. MMP2 conformation X (Table II) of (*S*)-**2** was used as starting geometry when τ_3 and τ_4 was driven from 145° to −79° and from 44° to −73°, respectively. The boat conformations resulting from this experiment [both conformations were almost identical with MMP2 conformation XIII (Table II)] were used as starting geometries when τ_3 and τ_4, respectively, were driven in the reverse direction. However, when τ_4 was driven in this latter direction, a chair conformation, almost identical with MMP2 conformation I (Table II), was obtained instead of the desired twist conformation. Therefore, we used a starting conformation having $\tau_4 = -43°$ when driving τ_4 toward 44°.

conformations of (*S*)-**2**.[32] Such conformations exist on the conformational interconversion path between the twist and boat conformation (conformation X and XIII; Table II). When expressed in τ_4[τ(C6,C7,C8,C9)], conformations of (*S*)-1 with τ_4 values from 11° to −1° might be able to activate the DA D_2 receptors since they fulfill the distance criteria given above (Figure 6). In the torsion angle driver method, geometries and energies of conformations are calculated along a potential energy path which is defined by one or several specific torsion angles. Initially, the torsion angle τ_3 = (C4a,C5,C6,N) was chosen as the reaction coordinate, and steric energies (MMP2) were calculated for τ_3 values from 145° (conformation X; Table II) to −149° in 3° increments, and from −149° to −79° (conformation XIII; Table II) in 10° increments. AM1 calculations were also performed by using the one bond driver technique. In these latter calculations, a smaller number of calculations were performed; τ_3 was driven in 3° increments between 154° and −167° in both directions.

The MMP2 potential energy profile resulting from an incremental change of τ_3 consisted of two different reaction paths. When τ_3 was driven from 145° to −79°, the steric energies increased steadily until $\tau_3 = -167°$ where a sharp drop in energy (−3.1 kcal/mol) and a major geometrical reorganization was observed (Figure 7a and Figure 8a,b). A different conformational path was obtained when τ_3 was driven in the reverse direction (−79° to 145°; Figure 7a).[33]

(32) In order to obtain conformations of (*R*)-**2** having the correct intramolecular distances (compare Figure 6), τ_1 was driven between the twist and boat conformations. This gave the same discontinuous energy profile as obtained when driving τ_3 in (*S*)-**2**. The relative saddle point energies were 7.9 kcal/mol when driving τ_1 from 136° to −126° and 6.9 kcal/mol when driving τ_1 in the reverse direction.

(33) The problem with discontinuous reaction paths has also been observed by other authors; see: (a) Anet, F. A. L.; Krane, J. *Tetrahedron Lett.* **1973**, 5029–5032. (b) Osava, E. *J. Am. Chem. Soc.* **1979**, *101*, 5523–5529. (c) Baas, J. M. A.; van de Graaf, B.; van Veen, A.; Wepster, B. M. *Recl. Trav. Chim. Pays-Bas* **1980**, *99*, 228–233. (d) Osawa, E. *J. Comput. Chem.* **1982**, *3*, 400–406. (e) Jaime, C.; Rubiralta, M.; Feliz, M.; Giralt, E. *J. Org. Chem.* **1986**, *51*, 3951–3955.

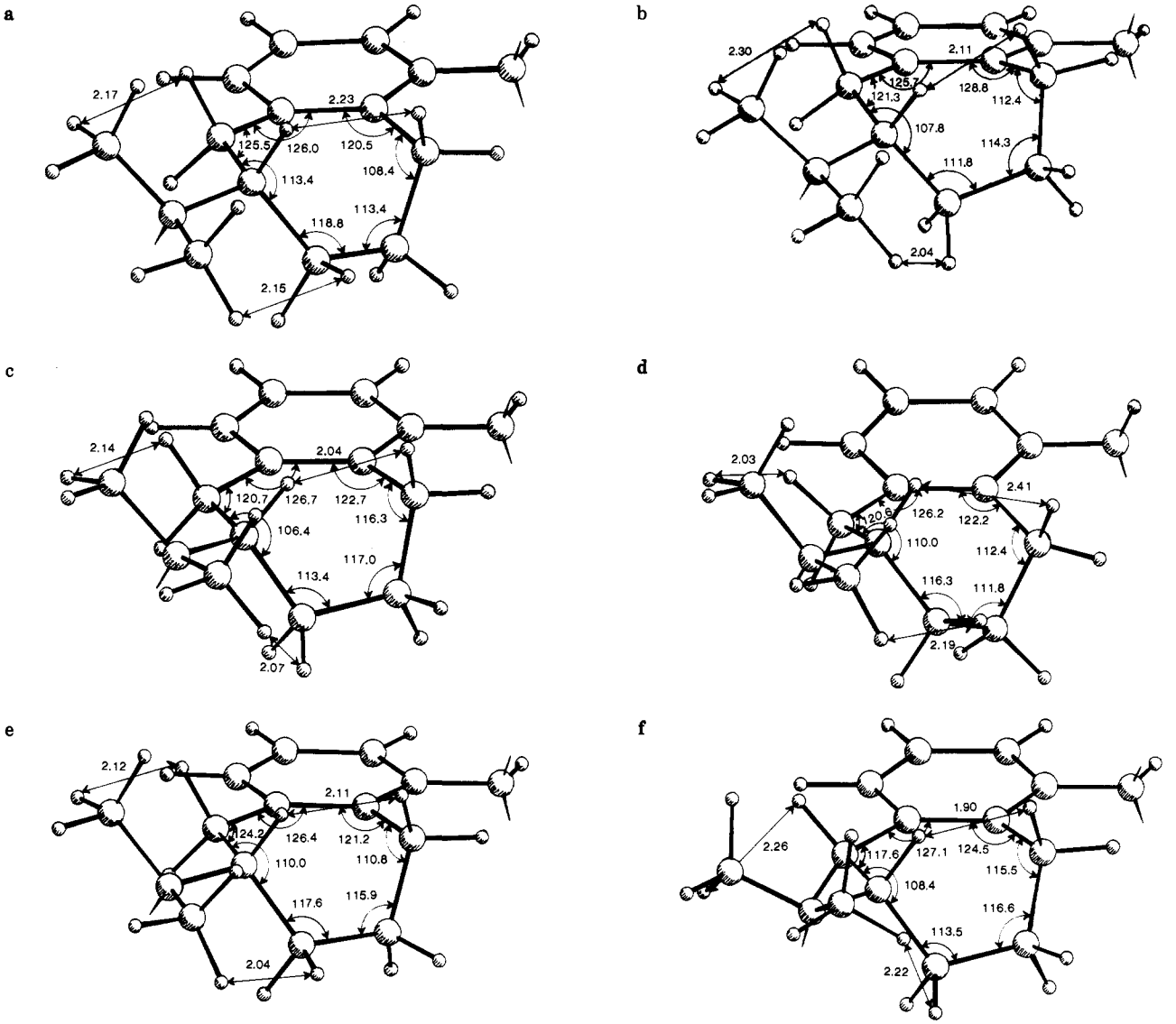

Figure 8. Comparison of valence angles (deg) and intramolecular distances (Å) of selected MMP2 and AM1 conformations along the calculated twist ↔ boat interconversion pathway of (*S*)-**2**. Conformations a and b correspond to geometries before and after the energy drop when driving τ_3 in the forward (twist → boat) direction, and conformations c and d correspond to geometries before and after the energy drop when driving τ_3 in the reverse direction. Conformation e was obtained by driving τ_4 and corresponds to one of the high-energy conformations (τ_4 = 5.0°; compare Figure 7d). Conformation f corresponds to the highest energy conformer obtained when using the AM1 method (τ_3 = 172° and τ_N = 90°; compare Figure 9).

It appears that a conformational path passing over geometries in which the C6 and C9 carbons become eclipsed, i.e., τ_4 values around 0°, is avoided when τ_3 is driven; τ_4 changes from 28° to −38° and from − 20° to 45° when τ_3 is moved from −167° to −164° and from 169° to 166°, respectively (Figure 7a,b). The geometries before (a, c) and after (b, d) the major energy drop are shown in Figure 8. Some geometrical features of a–d are noteworthy, e.g., the C4a–C5–C6 angle is large in a and the distance between $H_{6\beta}$ and $H_{9\beta}$ is short in c. In addition, hydrogens on the *N*-methyl groups are in close contact with $H_{5\beta}$ and $H_{7\beta}$ in b–d. The distance between $H_{6\beta}$ and $H_{9\beta}$ decreases from 2.23 Å to 2.11 Å, when **2** rearranges from the high- to the low-energy state (a and b, respectively). Inspection of the different energetical components contributing to the final steric energies revealed that the major energetical differences between conformations a and b were the bond angle bending term energies for the C4a–C5–C6 and C6–C7–C8 valence angles. These energies decreased by 1.1 and 0.8 kcal/mol, respectively, upon the molecular rearrangement.

For comparative purposes, the torsion angle τ_3 was driven in both directions between 154° and −167° by using the AM1 molecular orbital program and the one bond driver technique. Also with the AM1 program, two different conformational paths were obtained (Figure 9). However, this is due to drastic changes in τ_N values. An increase in τ_3 from 172° to 175° changed τ_N from 28° to −42°, and when τ_3 was decreased from 172° to 169°, τ_N changed from 90° to 161°. There are only minor deviations between the observed AM1 geometries and the corresponding MMP2 geometries (compare Figure 8).

Using the MMP2 program, we also studied the interconversion pathway between the twist and boat conformations with τ_4 as the reaction coordinate. τ_4 was driven in both directions in 3° increments between 44° and −43° and in 10° increments between −43° and −73° (Figure 7d). In contrast to the results obtained when τ_3 was driven, the one bond angle drive procedure using τ_4 gave a smooth and reversible path between 44° and −43°. However, when τ_4 was driven from −73°, a symmetrical mode of conformational interconversion,[34] leading to the chair conformation,

(34) Hendrickson, J. B. *J. Am. Chem. Soc.* **1964**, *86*, 4854–4866.

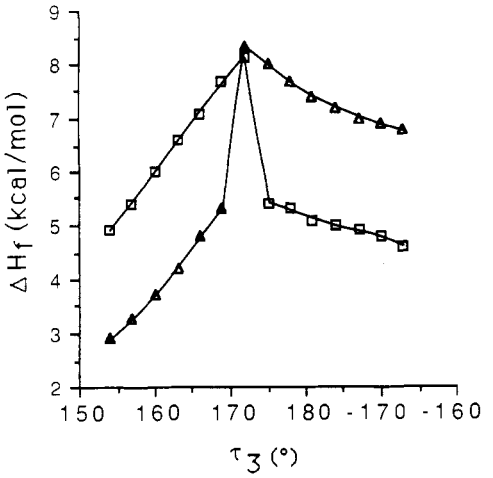

Figure 9. Calculated relative heats of formation (AM1) resulting from a change of the torsion angle τ_3 in 3° increments between 154° and −167° in both directions. Starting geometries were obtained from the MMP2 torsion angle driver experiment (compare Figure 7a). Starting geometry in the forward direction (□; 154° to −167°: τ_3 = 153.8°, τ_N = 51.2°, τ_2 = −141.6°, τ_4 = 45.9°). Starting geometry in the reverse direction (△; −167° to 154°): τ_3 = −166.8°, τ_N = 70.0°, τ_2 = −160.3°, τ_4 = −37.5°). The energy drop occurring at τ_3 = 172° is due to changes in τ_N. In the forward direction τ_N changed from 28° to −42° and in the reverse direction from 90° to 161°.

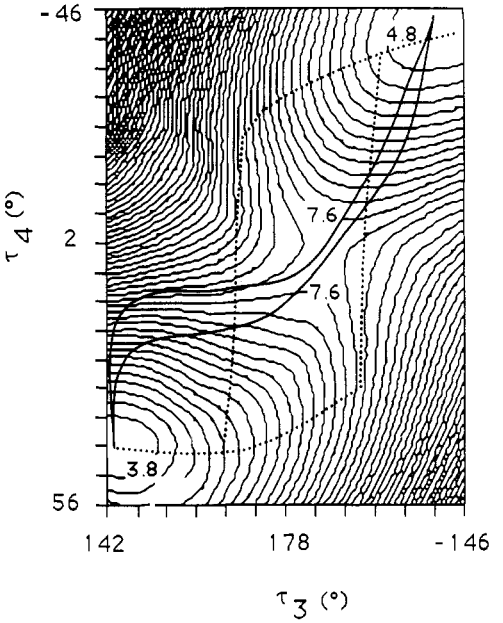

Figure 10. Torsional energy contour map and reaction pathways for conformational processes in (*S*)-**2**. MMP2 conformation X (Table II) was used as starting geometry, and the torsion angles τ_3 and τ_4 were driven in 6° increments. The reaction pathway obtained when driving τ_3 (dotted line) and τ_4 (solid line) and the concomitant changes in τ_4 and τ_3, respectively, are also indicated (compare with Figure 7). Steric energies (kcal/mol) are relative to conformation III (MMP2) of (*S*)-**2**. Contours are spaced at 0.25 kcal/mol.

was obtained (see also legend to Figure 7).

Although the use of τ_4 as the coordinate gave a smooth interconversion pathway with respect to τ_4, the observed changes in τ_3 appeared discontinous (Figure 7c). Therefore, we used the two-angle driver technique[35] to more fully explore the potential energy surface in the vicinity of potential DA D_2 pharmacophore conformations of the model compound (*S*)-**2**. The results of driving τ_3 against τ_4 is shown in Figure 10. When the results from the one bond drive technique are plotted, as in Figure 10, it is apparent that (*S*)-**2** passes nicely over the saddle point when τ_4 is used as the reaction coordinate. τ_4 appears to be a better suited internal coordinate than τ_3 for modelling the twist ↔ boat interconversion pathway of **2**. Figures 7d and 10 also demonstrate that, according to MMP2, pharmacophore conformations of (*S*)-**2** (τ_4 values between 11° and −1°) have steric energies 7.6–8.0 kcal/mol above that of the minimum energy conformation. The AM1 calculations indicate that such conformations have energies 7.4–8.3 kcal/mol above that of the global minimum.

Molecular Graphics Studies

To investigate if the identified pharmacophore conformations could be encompassed within the partial DA D_2 receptor excluded volume (Figure 1a) the different molecular volume maps were combined[36] by using the Chem-X and SYBYL molecular modelling systems. (*R*)-**2** produced a large excess volume—this volume might be part of the DA D_2 receptor essential volume (Figure 1c). (*S*)-**2** produced much less excess volume (Figure 1b). Most likely, this volume is of negligible biological significance since the excess volume due to $H_{9\alpha}$ occupies space in a narrow cavity formed by the receptor-excluded volume. The excess volume close to the nitrogen atom should also be acceptable to the receptor (this part of the volume is poorly defined in the model since we use methyl substituents instead of propyl groups).

Concluding Remarks

The observation that MMP2 and AM1 calculations of geometries and energies of the free base of **1** gave results that agree with the NMR spectroscopic study of **1**·HBr makes it reasonable to assume that also the calculations on the bioactive conformations are reliable. Thus, pharmacophore conformations of (*S*)-**1** seem to be energetically disfavored with about 7–8 kcal/mol. The molecular graphics studies indicate that pharmacophore conformations of (*S*)-**2** do not produce volumes that are part of the DA D_2 receptor essential volume. Taken together, the present results indicate that it should be impossible to design DA D_2 receptor agonists of the benzocycloheptenylamine class.

The model used in the present report—a flexible pharmacophore in combination with a partial receptor-excluded volume—may turn out to be very useful. It might, e.g., be applied in the design of new target compounds for synthesis and testing. However, we have not strictly defined the geometrical limits within which the pharmacophore can vary. This would require access to additional, and preferentially rigid, inactive compounds that do not produce excess volume in relation to the receptor-excluded volume. Similarly, we have not been able to define the flexibility of the receptor-excluded volume. This is another complicating consequence of the flexibility of the receptor protein.

(35) For a discussion of the advantage of using two torsion angles instead of one, when studying conformational processes, see ref 33d.

(36) The SET MAP option was used in Chem-X. The van der Waals volumes of the four molecules defining the partial DA D_2 receptor excluded volume and the selected conformations of (*S*)-**2** or (*R*)-**2** were combined by using the logical command OR. The DA D_2 receptor excluded volume was then subtracted by use of the command EOR. The map was contoured at the van der Waals level with a grid size of 24^3 and a significance level of 0.95. This procedure defines the excess volume produced by each of the enantiomers. The SYBYL molecular combination procedure is described in the legend to Figure 1.

Acknowledgment. We thank Dr. Tommy Liljefors and Dr. Robert E. Carter for providing access to the MIMIC program. Peter Szmulik, Department of Organic Chemistry, KTH, Stockholm, is gratefully acknowledged for helping us to produce the stereodrawings in Figure 1 with the molecular modelling system SYBYL, TRIPOS Associates, Inc., 6548 Clayton Road, St. Louis, MO 63117. The financial support from The Swedish Natural Science Research Council, Centrala Försöksdjursnämnden, The Royal Swedish Academy of Sciences, and IngaBritt and Arne Lundbergs Forskningsstiftelse is gratefully acknowledged.

Registry No. 1, 78950-88-6; (*S*)-1, 119208-12-7; (*R*)-1, 119208-13-8; (*S*)-2, 119184-58-6.

Synthesis, DNA-Binding Properties, and Antitumor Activity of Novel Distamycin Derivatives

Federico Maria Arcamone,* Fabio Animati, Brunella Barbieri, Emanuela Configliacchi, Roberto D'Alessio, Cristina Geroni, Fernando Carlo Giuliani, Ettore Lazzari, Milena Menozzi, Nicola Mongelli,* Sergio Penco, and Maria Antonietta Verini

Research and Development, Farmitalia-Carlo Erba, Erbamont Group, Milan, Italy. *Received April 29, 1988*

A group of potential alkylating agents have been synthesized that are structurally related to the oligopeptide antiviral antibiotic distamycin. All derivatives form complexes with native calf-thymus DNA but compounds **2**, **3**, and **6** give rise to covalent adducts. Cytostatic activity against both human and murine tumor cell lines in vitro is displayed by the new compounds. Compounds **3** and **4** are active on melphalan-resistant L1210 leukemia in mice.

Compounds endowed with the property of interacting directly with the nucleic acids are of great importance in cancer chemotherapy.[1] They may be divided into (a) compounds that are able to bind covalently to cell DNA (such as the alkylating agents), (b) agents that cause the breakage of the DNA molecule (such as the bleomycins and streptonigrin), and (c) drugs that bind reversibly to double-helical B DNA either by intercalation (such as the anthracyclines and the acridines) or by an external binding mode in the minor groove (such as the distamycins and netropsin).[2] Also in the case of reversible complexing agents, however, chemical reaction leading to irreversible damage of the DNA has been considered as the basis of the high antiproliferative effect of the same.[3] It appears therefore that the final effect exerted by drugs at the DNA level may be the result of different mechanisms related with the target recognition properties and the chemical reactivity of the different compounds. Distamycin (distamycin A, stallimycin, 1), an antiviral compound originally isolated from the cultures of *Streptomyces distallicus*,[4] is endowed with high affinity for AT-rich sequences of B DNA and the corresponding drug–DNA complex has been the object of extended studies.[5] We wish to report the synthesis and some properties of distamycin derivatives and analogues containing a chemically reactive appendage at the N-terminus. The compounds **2–6** represent a novel series of potential anticancer agents as it is shown by their ability to inhibit tumor cell proliferation in vitro and in vivo.

Compound **2** was obtained from *N*-deformyldistamycin (**7**), which was prepared from distamycin according to the already reported procedure.[6] Compound **7** was converted to **2** by reaction with ethylene oxide to give *N*,*N*-bis(2-hydroxyethyl) derivative **8**, which gave the corresponding *N*,*N*-bis(2-chloroethyl) derivative when treated with mesyl chloride in pyridine (Scheme I). Synthesis of **3** was similarly accomplished with **9a** as the starting material (ref 7). Compounds **4** and **5** were obtained from **7** with respectively **12** and **13a** as acylating agents. Analogue **6** was synthesized from **9b** (ref 7), which was reduced to the amine **10b** and converted to the *N*,*N*-bis(2-chloroethyl) derivative according to the procedure shown in Scheme

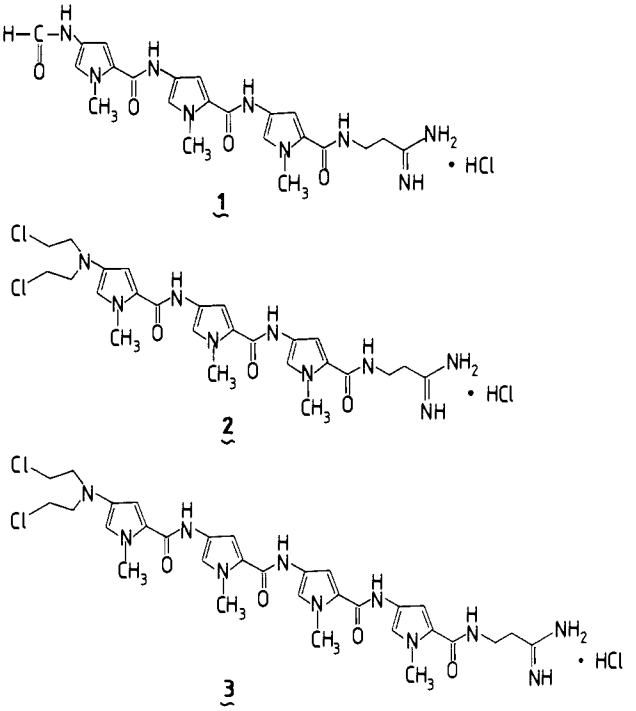

1

2

3

(1) Neidle, S., Waring, M. J., Eds. *Molecular Aspects of Anticancer Drug Action*; Macmillan: London, 1983.
(2) Waring, M. J. *Drugs Exp. Clin. Res.* **1986**, *12*, 441.
(3) Zwelling, L. A. *Cancer Metastasis Rev.* **1985**, *4*, 263.
(4) Arcamone, F.; Penco, S.; Orezzi, P. G.; Nicolella, V.; Pirelli, A. *Nature* **1964**, *203*, 1064.
(5) For a comprehensive review on the structure and physicochemical properties of the distamycin–DNA complex and the applications of the antibiotic in molecular biology and in genetic analysis, see: Zimmer, Ch.; Waehnert, V. *Prog. Biophys. Mol. Biol.* **1986**, *47*, 31.
(6) Arcamone, F.; Orezzi, P. G.; Barbieri, W.; Nicolella, V.; Penco, S. *Gazz. Chim. Ital.* **1967**, *97*, 1097.
(7) Arcamone, F. Nicolella, V.; Penco, S.; Redaelli, S. *Gazz. Chim. Ital.* **1969**, *99*, 632.

0022-2623/89/1832-0774$01.50/0